Investigating the Effects of Vps45 Mutations Associated with Severe Congenital Neutropenia on SNARE Interactions

A Major Qualifying Project Report
submitted to the Faculty of
WORCESTER POLYTECHNIC INSTITUTE
in partial fulfilment of the requirements for
the degree of Bachelor of Science

By:
Alexandra D'Ordine
Biochemistry & Professional Writing

Date:
27 April 2017

Report Submitted to:

Professor Mary Munson
University of Massachusetts Medical School

Professor Destin Heilman
Worcester Polytechnic Institute

Abstract

Vps45 is a Sec1/Munc18-like (SM) protein that regulates SNARE complex formation for endosomal vesicle fusion. In yeast, Vps45 has been shown to interact with its binding partner SNARE Tlg2, the yeast homolog of mammalian syntaxin 16 (Sx16), to control its entry into the SNARE complex. Recent studies have identified two independent single amino acid substitutions in Vps45 associated with the immune disorder severe congenital neutropenia. This study used *in vitro* binding assays to show that the human Vps45 mutants interact with the cytoplasmic portions of Sx16 and Tlg2 comparably to the wild-type, but one mutant may associate less strongly with truncations. Future research should use the assays demonstrated in this study to further test the affinity between mutated Vps45 and truncations of its binding partners, as well as association with the SNARE complex as a whole, to suggest a molecular mechanism for the disease.

Acknowledgments

Thank you to everyone who contributed to the development, advisement, and completion of this project. I would like to acknowledge the following individuals:

- Dr. Mary Munson for allowing me the opportunity to complete exciting biochemical research as a member of her lab, advising this project, and serving as a mentor to help me grow as a scientist.
- Dr. Destin Heilman for also advising this project and providing feedback on writing this report and creating the poster.
- Dr. Lorraine Higgins for advising the Professional Writing portion of this interdisciplinary MQP.
- Dr. Dante Lepore for helping me design and troubleshoot experiments.
- Other members of the Munson lab for their insight and support: Anne Mirza, Robert Orr, Rachael Heard, Allison Butt, Kristyn Norris, and Benjamin Crawford.
- Dr. Peter Newburger and other members of the Newburger lab for their collaboration: Zhiqing Zhu, Kimberly Ng, and Josias BritoFrazao.

Table of Contents

Introduction

Cellular homeostasis is maintained through many complex processes. These include energy production, DNA maintenance, gene expression, protein folding, and molecular transport. One mechanism of transport uses vesicles, lipid bilayer-enclosed compartments, to move various types of cargo into, out of, and around the cell. This includes proteins that are translated and folded in the endoplasmic reticulum, sorted in the Golgi apparatus, and packaged into vesicles to function at the plasma membrane or be secreted outside the cell in the exocytic pathway [1]. Macromolecules, signaling molecules, and other materials are brought into the cell for recycling or degradation in the endocytic pathway [1]. Due to the many types of cargo and functions of vesicles as a whole, specialized proteins participate in and regulate each process [1]. In addition, these proteins are highly conserved in eukaryotes from the single-celled yeast *Saccharomyces cerevisiae* to mammals [1]. Therefore, vesicle trafficking is an essential activity for the growth and overall survival of cells.

Vesicle Transport Pathways and Associated Proteins

Vesicle transport includes several common steps regardless of the specific pathway it functions in within the cell. First, vesicle formation is initiated when coat proteins, such as clathrin or coat protein complexes (COPI and COP II), are brought to the site of budding by GTPases or lipids within the membrane [1]. SNARE proteins and transmembrane cargo proteins also gather at the budding vesicle [1]. Next, the vesicle must bud from its initial compartment, such as the endoplasmic reticulum, containing only the correct cargo as designated by sorting motifs or other tags [1,2] . The protein coat polymerizes in order to create the membrane curvature needed to begin separating the emerging vesicle from the donor membrane [1,2]. The newly-formed vesicle's lipid composition, as well as the cytoskeleton, can also promote vesicle formation [1,2].

Vesicle fission occurs next in order to completely separate the vesicle from the donor membrane, which can be mediated by the GTPase dynamin [2]. The protein coat used for budding is no longer needed once fission has occurred, so the coat proteins are removed by uncoating proteins and then recycled [1]. Microtubule or actin motor proteins, such as myosins, then selectively move the vesicle to the target membrane [2]. Once it approaches its destination, the vesicle becomes tethered by GTP-bound Rabs and other tethering factors [1,3]. During docking, the vesicle is close enough to the target membrane to allow the soluble N-ethylmaleimide-sensitive factor attachment protein receptor (SNARE) proteins attached to the vesicle membrane and the target membrane to form the SNARE complex in a highly regulated process [1]. Finally, fusion occurs when the SNARE complex brings the vesicle and target membranes together to form a single compartment, allowing the cargo to diffuse to its destination [2].

One general vesicle transport pathway is the endocytic pathway in which materials are brought into the cell. Vesicles coated in clathrin or caveolin bud from the plasma membrane carrying various types of cargo from outside the cell or that are embedded in the membrane itself [2]. Extracellular fluids are brought in using macropinosomes [2]. Certain cells, such as white blood cells like macrophages and neutrophils, also engulf large materials, such as bacteria, in phagosomes or phagolysosomes [2]. Following internalization, the vesicles fuse with early endosomes, membrane-enclosed compartments located in the cytoplasm, and the contents sorted into one of three potential pathways [2]. Cargo can be sent directly to the plasma membrane, to recycling endosomes before returning to the plasma membrane or being transported to the *trans*-Golgi for further sorting, or to late endosomes which can lead to the Golgi or lysosomes, organelles that digest cellular debris [2].

As described above, in order to regulate vesicle movement and fusion, several classes of proteins associate with vesicles. SNAREs attach to vesicle (v-SNAREs) or target membranes (t-SNAREs) through their C-terminal transmembrane domain [1]. Many different types of SNAREs exist, with 38 found in humans, but they all share a helical coiled-coil SNARE motif and a transmembrane domain [3]. SNAREs can also be further categorized into R-SNAREs and Q-SNAREs that contain a central arginine or glutamine, respectively, in this helical motif; most R-SNAREs are also v-SNAREs while most Q-SNAREs are t-SNAREs [3]. Other common motifs for syntaxins, one type of t-SNARE, include the regulatory N-peptide and autoinhibitory H_{abc} domain, as shown in Fig. 1A [3]. During vesicle docking, one v-SNARE and three t-SNARE helices form a twisted bundle called the *trans*-SNARE complex through their SNARE motifs, which brings the membranes together to promote fusion [3,4]. Following fusion, the complex left on the fused membrane is known as the *cis*- SNARE complex [3]. The SNAREs are then recycled by the ATPase N-ethylmaleimide-sensitive factor (NSF) and soluble NSF attachment proteins (SNAPs) [4]. In addition, Rab GTPases and tethering complexes, such as the exocyst complex, coordinate SNARE arrangement and vesicle fusion [3,4].

Additional proteins are required to ensure specific and accurate SNARE complex assembly, including Sec1/Munc18 (SM) proteins. These peripheral membrane proteins interact with SNAREs to regulate SNARE complex assembly and membrane fusion [4]. In order to keep distinct vesicle transport processes separate, certain SM proteins are associated with each pathway and can be divided into four families based on their localization within the cell. Sly1 is involved in transport between the endoplasmic reticulum and the Golgi apparatus, whereas Mun18 (Sec1 in yeast) can be found at the plasma membrane [3]. Vps33 functions in the endosomal and lysosomal pathways, and Vps45 has been associated with endosomal trafficking

[3]. Seven SM proteins are found in total in vertebrates, but only four in yeast [5]. These proteins are conserved across their 600-700 amino acid length, with a common arch shape consisting of three domains, a hydrophobic pocket, and a central cleft, as shown in Fig. 1B and 1C [6]. This flexible groove allows the proteins to bind to SNAREs, predominately with syntaxins. The SM protein's central cleft can bind to the closed conformation of syntaxins, which exists when the H_{abc} domain binds to the SNARE motif [4]. SM proteins can also bind to the N-peptide of syntaxins via a hydrophobic pocket, which is the more common and higher affinity form of association [7]. Since syntaxins cannot participate in the SNARE complex when the H_{abc} domain binds to the SNARE motif, SM proteins can promote opening of syntaxins for complex formation [6]. They also can interact with other SNAREs and the assembled SNARE complex [4].

SM proteins may also play a role not only in SNARE complex formation, but during membrane fusion. They can remain attached to the complex through the N-peptide of their associated syntaxin or by directly binding to the helical bundle [4]. SM proteins also have been shown to be required for the lipid mixing that occurs between the vesicle and target membranes when they fuse [4]. Two potential models exist to explain how SM proteins interact with SNAREs to promote membrane fusion. The first suggests that they prevent SNAREs from diffusing into the space between the two membranes, which could physically bar fusion [4]. The second states that they destabilize the membrane fusion intermediate to favor complete fusion [4]. Despite the sequence conservation, the interactions between different SM proteins and their associated SNAREs vary; in some cases they can promote complex assembly while in others they prevent it, making a unifying functional explanation elusive [4].

Vps45 and Its Binding Partners

Vps45 is a 67 kDa SM protein that regulates endosomal trafficking. Vps45 is important for the transport of newly translated proteins and those that must be recycled to the plasma membrane, as well as the lysosomal pathway [8]. The protein is named for the vacuolar protein sorting defect found in the deletion mutant in yeast, in which the vacuolar enzyme carboxypeptidase (CPY) is secreted instead of transported to the vacuole [6]. In addition, the cells grow more slowly and vesicle accumulation occurs [8]. Vps45's cognate t-SNARE syntaxin is Tlg2 in yeast and syntaxin 16 (Sx16) in mammals, both of which are associated with the late Golgi [7,9].

Vps45 can bind to Tlg2 (or Sx16) through two modes, as shown in Fig. 1B and 1C. Vps45 contains a hydrophobic pocket in domain 1 that allows binding to Tlg2's N-peptide [6]. When this site is disrupted by the L117R substitution, Tlg2 no longer binds to the SNARE complex, as the mutation interferes with binding to the open conformation of Tlg2 [6]. Analogously, the N-peptide of Sx16 also shows a strong, conserved affinity for mammalian Vps45 [10]. However, this interaction is not needed for normal membrane trafficking to occur [6]. Vps45's central cleft also interacts with the closed conformation of Tlg2. Tlg2's H_{abc} domain, SNARE motif, and linker sequence between the two regions are required for binding to Vps45's central cleft [7]. When Tlg2's H_{abc} domain binds to its SNARE motif, Tlg2 is considered to be in the closed conformation and is unable to participate in SNARE complex formation [7]. Vps45's binding to Tlg2 in this way has also been shown to stabilize this closed conformation [7]. In addition, Tlg2 has been shown to tightly interact with mammalian Vps45 and Sx16 with yeast Vps45, demonstrating binding between the homologs [10]. Also, residues outside of the hydrophobic pocket of mammalian Vps45 stabilize Sx16 binding [9]. In summary, Vps45's

hydrophobic pocket interacts with Tlg2/Sx16's N-peptide, whereas Vps45's central cleft interacts with Tlg2/Sx16's C-terminus (Fig. 1B and 1C) [7].

While either binding mode is sufficient for normal trafficking in yeast, when both interactions are disrupted the cell has a CPY sorting defect similar to the *TLG2* deletion [7]. In *TLG2* null yeast, mammalian Sx16 can restore function and remove the trafficking and growth defects [9]. A dominant negative gain-of-function Vps45 mutation, W244R, also causes the CPY sorting defect in yeast [6]. This mutant can only bind through the N-peptide, as it cannot bind to the truncation of Tlg2 lacking the N-peptide [6]. The conserved residues near this point mutation in domain 2 suggest that this mutation may lock Vps45 in an open conformation, preventing it from participating in the two modes of binding that are necessary during SNARE complex assembly and disassembly and potentially increasing its affinity for the assembled complex [6]. However, the two binding modes of Vps45 and Tlg2 are not independent of each other. Using truncations of Tlg2, it was demonstrated that the N-peptide competes with the closed conformation's ability to bind to the central cleft of Vps45, but only when the hydrophobic pocket is intact [7]. Therefore, the N-peptide participates in controlling the entry of Tlg2, or Sx16, into the SNARE complex [7].

Vps45 also binds to the yeast v-SNARE Snc2 and the assembled SNARE complex. Snc2, which also functions in exocytosis, does not require the hydrophobic pocket of Vps45 to bind [6,11]. However, Tlg2 can displace Snc2 for binding but Snc2 cannot replace Tlg2, suggesting that the binding sites are connected [7]. The Vps45 W244R mutant binds Snc2 more strongly than the wild type [6]. The resulting decrease in free Snc2 causes incorrect endosomal trafficking because expressing additional Snc2 restores the normal transport phenotype [11]. Vps45 associates with the SNARE complex through Tlg2's N-peptide, while the W244R mutant binds to the SNARE complex even when it includes Tlg2 without the N-peptide [6]. In addition, yeast Vps45 has also

been shown to affect the levels of Tlg2 and Snc2 *in vivo*; a decrease in Vps45 results in a comparable decrease in Tlg2 and Snc2 [11]. Similarly, levels of Sx16 decrease without Vps45 [9]. This could be caused by Vps45's stabilization of Tlg2, which suggests that less Vps45 would destabilize Tlg2 and decrease its concentration in the cell [11].

Severe Congenital Neutropenia and Vps45

Recently, two single amino acid mutations in Vps45 have been found in patients with severe congenital neutropenia (SCN), an immune disorder characterized by a neutrophil concentration below 0.2 x 10^9 per liter of blood and frequent bacterial infections [12]. Neutrophils are granulocytes that protect against infections by engulfing and neutralizing pathogenic bacteria [13]. They migrate to the location of infection and secrete antimicrobial proteins from specialized granules, as well as reactive oxygen species, in order to degrade bacteria in the phagosome or extracellularly [14]. Neutrophils also modulate the inflammatory response through cytokines, which recruit macrophages, T cells, and additional neutrophils [14]. After performing these functions, neutrophils commit apoptosis and are degraded by macrophages in order to avoid spilling proteolytic enzymes and reactive oxygen species into the inflamed tissue [14]. Neutrophils develop from myeloid stem cells in bone marrow [14]. These cells give rise to granulocyte-macrophage progenitors, which then mature into neutrophils or related cells based on differences in gene expression patterns [14]. Due to their low levels of neutrophils, individuals with SCN are susceptible to bacterial infections from infancy and require granulocyte colony-stimulating factor (G-CSF) treatment to promote the production of more and healthier neutrophils [15]. However, 20% of patients eventually develop myelodysplastic syndrome or acute myeloid leukemia [16]. Though G-CSF has been effective in 90% of cases, treatment could increase the already high risk of developing these secondary conditions [16].

While Rolf Kostmann first described severe congenital neutropenia in 1956, the underlying genetic cause of the disease has only recently been investigated [12]. SCN is a heterologous disease resulting from mutations in several different genes, with the genetic cause unknown in approximately 30% to 40% of patients [17,18]. The most common genetic cause of SCN is mutated *ELA2*/*ELANE*; around 50% of SCN patients have a mutation in this gene, which is inherited in an autosomal dominant manner in most cases [19]. *ELA2* encodes neutrophil elastase, a serine protease expressed at very high levels in neutrophils since it degrades receptors and cytokines to control the immune response [15]. The many distinct mutations in *ELA2* destabilize the protein so that it is unable to fold properly. This accumulation of nonfunctional protein triggers the unfolded protein response (UPR) in which translation is slowed and extra chaperones are employed to reduce endoplasmic reticulum stress [19]. Due to the large amount of unfolded protein, the mutated neutrophil elastase often ultimately results in apoptosis in neutrophil precursors and neutrophils.

Mutations in most other genes that cause SCN, however, are autosomal recessive. For example, autosomal recessive *HAX1* mutations were identified through pedigree analysis [20], and have been found in 11% of patients in the European Severe Chronic Neutropenia Registry [15]. Mutations in *HAX1* were shown to cause a loss of mitochondrial membrane potential in neutrophils, resulting in apoptosis [20]. In addition to the SCN phenotype, neurological symptoms have been described in some patients with mutated *HAX1* [20]. Another gene associated with SCN that is not directly related to neutrophil activity is *G6PC3*, which affects approximately 4% of patients in the European Severe Chronic Neutropenia Registry [15,17]. These mutations also result in the UPR, disrupt proper glucose metabolism, and cause a decrease in the protein Mcl1 that normally prevents apoptosis [17].

Most recently, mutations in *VPS45* in seven distinct families have been associated with SCN, designated as SCN5 [21]. In all cases the mutation was inherited in an autosomal recessive manner [13]. First, a T224N mutation was identified in five affected Palestinian families using homozygosity mapping, exome sequencing, and pathogenicity prediction software [8]. When a plasmid containing the corresponding yeast Vps45 mutation, T238N, was expressed in a yeast strain lacking wild-type Vps45, levels of Vps45 and Tlg2 decreased by around 44%, indicating that the mutation destabilizes the protein [8]. The patients' cells showed lysosome depletion and a decrease in α granules in platelets, as well as increased apoptosis of neutrophils and myeloid cells [8]. The five patients not only showed symptoms of severe congenital neutropenia, but of primary myelofibrosis (ineffective blood stem cell differentiation), and bone marrow failure [8]. Two died of infections, two were waiting for bone marrow transplants at the time of publication, and the last began exhibiting normal neutrophil counts after a bone marrow transplant [8]. Five other patients with this mutation have also been identified [13]. Studies from these patients' cells showed a similar decrease in the amount of Vps45, as well as impaired localization of the protein throughout neutrophils [13]. They also found less β1 integrin, which functions in cell motility, on the surface of affected neutrophils and fibroblasts, as well as decreased levels of Sx16 and rabenosyn-5, which localizes Sx16 and promotes β1 integrin recycling [13]. Also, another Vps45 mutation, E238K, (E252K in yeast) was found in two Moroccan families [13,21]. One family had two affected children who died of infections during infancy [13]. Another family's affected child received a successful bone marrow transplant at 18 months [21]. Like *HAX1* mutations, the E238K mutation has been associated with neurological abnormalities and impaired vision [13,21]. Successful bone marrow transplants have been reported for a total of four patients with Vps45 mutations [21].

However, the pathway by which mutations in Vps45 cause SCN remains unknown. Though it is unclear exactly why neutrophils are affected by these mutations while other related immune cells are not, the Vps45 transcript is expressed the most in neutrophils and peripheral blood mononuclear cells [8]. In a structural model of Vps45, both of these mutations were found in the central cleft of the protein; these mutations were predicted to potentially destabilize the protein and prevent it from functioning properly [13]. Some studies have suggested that the accumulation of incorrectly sorted vesicles in the absence of functional Vps45 results in neutrophil apoptosis by triggering the UPR due to endoplasmic reticulum stress [8]. However, other studies have observed no endoplasmic reticulum stress [13]. Instead the impaired transport of proteins in neutrophils combined with their high turnover rate, propensity for apoptosis, and lack of expression of the apoptosis-preventing protein Bcl-2 could cause their tendency to undergo apoptosis [13]. Understanding how these Vps45 mutations cause SCN is crucial because no patients studied have responded to the G-CSF treatment, and some have not survived after bone marrow transplants [8,13,21].

This project investigated the binding of Vps45 to Tlg2 and Sx16. The wild-type interactions between yeast Vps45 (yVps45) and Tlg2 without the N-peptide were assayed using size-exclusion chromatography and native gels to allow for comparison to mutated yVps45 in the future. The results from pulldown assays of human Vps45 (hVps45) suggest that though the mutants show no observable difference in binding to the full cytoplasmic portion of Tlg2/Sx16, there may be a difference in binding to Tlg2/Sx16 without the N-peptide for at least one of the mutants. While improved pulldown assay conditions and additional methods are needed to support this hypothesis, this project has demonstrated several assays that can show binding between Vps45 and Tlg2/Sx16 and that should be used to further characterize the Vps45

mutants. Future studies should also test the effects of the mutations on SNARE complex binding as a whole. By observing any differences in affinity or behavior when comparing the wild-type and mutants, we may be able to better understand how these Vps45 mutations cause severe congenital neutropenia.

Methods

Construct Design

Bacterial Expression Constructs

QuikChange site-directed mutagenesis (Agilent) was used to introduce mutations in the His-tagged *S. cerevisiae* Vps45 gene in pMM446, an *E. coli* expression plasmid with the pETDuet-1 backbone and ampicillin resistance. The T238N mutation was created by substituting 713C→A and 714A→C, counting from the start codon, using primers Vps45_T238N_F (5'-GTAATACTGATCCTATAAACCCTTTACTTCAACCTTG-3') and Vps45_E252K_R (5'-CAAGGTTGAAGTAAAGGGTTTATAGGATCAGTATTAC-3'). The E252K mutation was created by substituting 753G→A using primers Vps45_E252K_F (5'-CCAATCAATGATCAATAAGTATATAGGCATTAAGC-3') and Vps45_E252K_R (5'-GCTTAATGCCTATATACTTATTGATCATTGATTGG-3').The 50µL PCR reaction contained the following components: 5µL of 10X Pfu Ultra HF Reaction Buffer AD, 4µL of 2.5mM dNTPs, 100ng of template DNA (~1µL), 0.5µL of each primer, 1µL of Pfu Ultra High-Fidelity DNA Polymerase AD, and sterile water to 50µL. The PCR program used contained the following steps: 1.) 1 min at 95 °C, 2.) 30 sec at 95 °C, 3.) 30 sec at 55 °C, 4.) 8 min at 72 °C (based on the ~8kb size of the plasmid), 5.) steps 2-4 repeated 30 times, and 6.) 10 min at 72 °C. The reaction was incubated with 0.96µL of DpnI at 37 °C for 2 hr to remove the template plasmid and then 2µL was transformed into DH5α competent cells and grown overnight on LB + carbenicillin plates. Plasmids from individual clones were extracted using Qiagen's Miniprep Kit and tested for the mutation by sequencing.

The Sx16(28-280)-PrA expression plasmid was created by amplifying the applicable portion of the gene from pMM663 (Sx16(1-280)-PrA in pETDuet-1, from Gwyn Gould's lab) using primers with an NdeI restriction site (5'- GCGCGGCAGCCATATGCTTGCTGATGACC

GTATGGCAC-3') and XhoI restriction site (5'-GAACCAGCTCGAGTTTCCGATTCTTCTTT TGATAC-3'). The 50µL PCR reaction contained 4µL of 2.5mM dNTPs, 1µL of each primer, 1µL of a 1:25 dilution of the pMM663, 5µL of 10X Buffer, 1µL of Phusion Taq, and sterile water to 50µL. The PCR program used was as follows: 1.) 1 min at 98 °C, 2.) 30 sec at 98 °C, 3.) 30 sec at 52 °C, 4.) 30 sec at 72 °C, 5.) steps 2-4 repeated 34 times, and 6.) 10 min at 72 °C. The PCR product was purified from the appropriate 0.8% agarose gel band using the QIAQuick Gel Extraction Kit. To digest the vector plasmid, also pMM663, 1µg of plasmid, 0.5µL of 100X BSA, 5µL of NEB Buffer 3.1, 1µL of NdeI, 1µL of XhoI, and 41.5µL of sterile water were incubated at 37C for 2 hr then gel purified as above. 1µg of the PCR product was digested similarly, but for 1 hr and purified with the QIAQuick PCR Purification Kit. The 20µL ligation reactions contained a 3:1 ratio of insert to vector with 80ng of vector, 2µL of 10X ligase buffer, 1µL of T4 DNA ligase, and sterile water to 20µL. The reaction was incubated at room temperature for 10 min, heated at 60 °C for 10 min, and transformed into DH5α competent cells alongside a control transformation with an equivalent amount of digested but not ligated plasmid. Colony PCR screening was performed and positive clones confirmed by sequencing.

Yeast Expression Constructs

Restriction digest cloning was performed to introduce the mutated yeast Vps45 genes from the *E. coli* expression plasmids into pPP450 (from Peter Pryciak's lab), a yeast expression plasmid with the pRS315 backbone (GAL promoter and leucine selection). Primers containing restriction sites for PstI (5'-GATCCCCCGGGCTGCAGATGGGCAGCAGCCATCAC-3') and XhoI (5'-CGGATTCCCCCTCGAGTTATTTTGCAGATCTAATAGAATCCATATATTCTTT AG-3') were used to amplify the genes. The PCR was performed, purified, and digested as described above but with the applicable templates and enzymes (PstI and XhoI), an annealing

temperature of 48 °C for the E252K mutant gene, and an extension time of 1 min. The plasmid was also digested as described above. The sample was gel purified using the QIAQuick Gel Extraction Kit. The ligation was performed as above, an analytical digest with EcoRV was used to check for the insert, and positive clones were confirmed by sequencing.

Protein Purification

Bacterial Growth

Wild-type yVps45 was purified using BL21 (DE3) competent cells with the plasmid containing GroEL/ES (pJK213 from J. Kahana, chloramphenicol resistance) thawed on ice and transformed with 2-3µL of pMM446 for 45 min on ice. His-tagged hVps45 in pET15b (pMM643 for wild-type, pMM641 for T224N mutation, and pMM642 for E238K mutation) was transformed similarly. The cells were grown overnight at 37 °C on LB + carbenicillin + chloramphenicol plates and then in liquid culture at 37 °C until the OD_{600} reached between 0.3 and 0.4, when flasks were shifted to 15 °C. Once the OD_{600} reached between 0.6 and 0.8, the cells were induced with 1mM IPTG and grown overnight. After 16-20 hr, cells were harvested by spinning at 5,000 rpm for 10 min at 4 °C. His-tagged Tlg2(37-318) (pMM464) was grown with this protocol, but using regular BL21 (DE3) competent cells and 0.1mM IPTG. Tlg2(1-309)-PrA (pCOG025 from Nia Bryant's lab), Sx16(1-280)-PrA (from Gwyn Gould's lab), Tlg2(37-309)-PrA (pCOG026 from Nia Bryant's lab), Sx4-PrA (from Gwyn Gould's lab), and Sx16(28-280)-PrA were also grown similarly but with codon+ BL21 (DE3) competent cells and 1mM IPTG.

Cell Lysis and Column Purification

The harvested 8L pellet of His-tagged Tlg2(37-318) or His-tagged yVps45 was either frozen at -80 °C for later purification or resuspended in 96mL of lysis buffer (300mM NaCl,

50mM NaH_2PO_4, 10% glycerol, 10mM imidazole, pH 8, with 1mM PMSF, 1 PIC tablet, 5mM β-mercaptoethanol, and a few flakes of lyophilized DNase added before use). The sample was lysed with 2 passes in a cell disrupter at 80psi. The lysate was spun at 13,000 rpm for 30 min at 4C.

Ni-NTA Agarose slurry (Qiagen) was used for affinity purification of His-tagged proteins. 2-5mL of a 50% slurry was washed with lysis buffer and centrifuged at 800 rpm for 3 min at 4 °C. The lysate supernatant was added to the beads and incubated with rocking for 1 hr at 4 °C. The beads were spun at 800 rpm for 3 min and most of the supernatant removed. After allowing the beads to pack, the column was washed with 100mL of wash buffer (300mM NaCl, 50mM NaH_2PO_4, 10% glycerol, 20mM imidazole, pH 8, with 5mM β-mercaptoethanol added before use) and then eluted with 16-25mL of elution buffer (300mM NaCl, 50mM NaH_2PO_4, 10% glycerol, 200mM imidazole, pH 8, with 5mM β-mercaptoethanol added before use) in ~1mL fractions. 5μL of each fraction was applied to Whatman filter paper and protein content visualized using Coomassie stain. The fractions with the most protein were pooled and slowly diluted 1:6 with Buffer A (20mMTris, pH 8.5 for Vps45 or pH 8 for Tlg2, 10% glycerol, filtered and degassed, with 1mM DTT added before use) and filtered for further purification using the Mono Q 5/50 GL anion-exchange column (GE). A gradient elution program was used from 5% to 50% Buffer B (Buffer A + 1M NaCl) over 20 column volumes (~20 mL). 0.5mL fractions were collected and gel samples were taken from each fraction corresponding to a peak. Protein samples taken throughout the purification process were run on an SDS-PAGE gel and visualized using Coomassie staining. Fractions containing the desired protein were pooled and concentrated. Aliquots were flash-frozen in liquid nitrogen and stored at -80 °C until use. Protein

concentrations were estimated using A_{280} with the protein's extinction coefficient and dilutions run on a gel compared with a GST standard.

Cell Lysis by Cryogenic Grinding

Pellets from 2L of His-tagged hVps45 (wild-type, T224N, and E238K), Tlg2(1-309)-PrA, Sx16(1-280)-PrA, Tlg2(37-309)-PrA, Sx4-PrA, and Sx16(28-280)-PrA were washed with 40mL of lysis buffer (same as above but without β-mercaptoethanol) and spun at 3,000 rpm for 20 min at 4 °C and the buffer removed. The pellets were then spun at 3,000 rpm for 15 min at 4 °C to remove excess buffer before freezing in noodles in liquid nitrogen and storing at -80 °C. The noodles were ground into powder with 6 cycles of cryogenic grinding at 400 rpm for 90 sec.

Yeast Transformation

To transform the yeast strain MMY654, a diploid strain ideal for protein expression, with the yVps45 yeast expression plasmids described above, a 5mL YPD culture was grown overnight at 25 °C and diluted to between OD_{600} 0.2-0.25 in a 30-50mL culture in the morning. The culture was grown until it doubled twice. 10 OD units of yeast were spun down at 3,000 rpm for 5 min, resuspended in 1mL of sterile water, and spun at 13,200 rpm for 2 min. Each reaction was resuspended in 345µL of transformation mixture (240µL of 50% PEG, 36µL of 1M lithium acetate, 20µL of salmon sperm DNA boiled for 5 min, and 49µL of sterile water) and 1-2µg of DNA added. The reaction was heated at 42 °C for 30-45 min, then spun at 13,200 rpm for 2 min and resuspended in 1mL of sterile water. 200µL was plated on each SC-Leu plate.

Yeast Growth and Small-Scale Induction

Transformed yeast colonies were grown in 5mL cultures of SC-Leu + 2% glucose overnight and diluted in 25mL of Sc-Leu + 2% glucose the following day. Cells were grown

until between OD_{600} 0.5 and 1 before being spun down, washed with 10mL of water, resuspended in SC-Leu + 2% galactose to induce, and grown overnight. 4 OD units were spun at 3,000 rpm for 5 min and the pellets washed with 1mL of water. The pellet was resuspended in 100µL of 0.1M sodium hydroxide and incubated on ice for 10 min. The sample was spun at 3,000 rpm for 2 min, and the pellet resuspended in 50µL of 1X SDS-PAGE loading dye and boiled for 5 min.

Western Blot Assay

Protein samples were run on an SDS-PAGE gel with a color protein marker. The protein was transferred to nitrocellulose, or PVDF washed with methanol for 10 min, at 100V for 1 hr at 4 °C. The blot was rinsed with PBS, blocked with 5% milk in 0.5% PBS-Tween (PBS-T) for 1 hr with rocking, and stored overnight at 4 °C (optional). The blot was washed with PBS until no milk remained. The blot was incubated with 10mL of primary antibody at the appropriate dilution (α-His 1:1000 (mouse), α-yVps45 1:1000 (mouse), α-hVps45 1:200 (rabbit), α-Sx16 1:2000 (rabbit), α-Sec1 1:1000 (rabbit), or α-Sso1 (1:2000)) in 0.5% PBS-T with 2% BSA for 1 hr with rocking. Three 10-min washes were performed with 0.5% PBS-T. The blot was incubated with an appropriate dilution of secondary antibody (1:5000 goat-α-mouse or 1:5000 goat-α-rabbit) in 5% milk in 0.5% PBS-T for 1 hr with rocking, followed by three 10-min washes with 0.5% PBS-T. 1mL of each of the two Western Blotting Substrate components was mixed and allowed to react with the blot for 1 min before visualizing by a 1 sec to 2 min exposure.

Binding Assays

Size-Exclusion Chromatography

150µL samples containing each protein (yVps45 and Tlg2(37-318)) individually and together diluted to the desired concentration with potassium phosphate buffer (10mM potassium phosphate, 140mM potassium chloride, pH 7.4, with 1mM DTT added before use) were spun at 13,200 rpm for 10 min at 4 °C. The samples were run on a Superdex 200 10/300 GL size-exclusion column (GE) and 0.5mL fractions collected during the elution of 1 column volume (~24mL). To precipitate 0.5µL of 20% trichloroacetic acid solution was added to each fraction and the sample incubated on ice for 30 min. The reactions were spun at 13,200 rpm for 10 min at 4 °C. The supernatant was removed, 1mL of acetone added, and the reaction mixed. After another spin as before, the acetone was removed and the pellet allowed to air dry. The pellet was resuspended in 1X SDS-PAGE loading dye and boiled for 5 min. Samples were loaded on a SDS-PAGE gel and visualized with Coomassie staining.

Native Gels

5X native gel buffer containing 43mM imidazole and 35mM HEPES was created at pH 7.4 and stored at 4 °C. One native gel with 6% acrylamide was poured using the following components: 2.4mL of 5X native gel buffer, 1.8mL of 40% acrylamide, 0.6mL of 50% glycerol, and 7.1mL of water, with 84µL of 10% APS and 8.5 µL of TEMED added just before pouring into 1.5mm spacer plates. The 6X loading buffer contained the following components for 1mL: 600µL of 1X native gel buffer, 300µL of 100% glycerol, 2.5mg of bromophenol blue, and 100µL of water. 20µL reactions of the proteins individually and at together at varying concentrations were incubated on ice for 45-60 min. The gel was run at constant amperage of 30mA for 15 min

at 4 °C before loading and then for 90 min after loading. The proteins were visualized using Coomassie staining.

Pulldown Assays

The powders for each protein were resuspended in 600uL of lysis buffer (40mM Tris, pH 8.0 and 200mM sodium citrate, with 1mM PMSF added before use) per 50mg of powder and resuspended by vortexting in 15-sec increments separated by 30 sec on ice until no clumps remained. The lysate was then spun at 13,000 rpm for 10 min at 4 °C. 5µL of magnetic beads conjugated with rabbit IgG were used per sample to bind to the PrA-tagged constructs. 10uL of beads were washed 3 times with 500µL of lysis buffer before being resuspended in 200µL of buffer and split between the control and experimental tubes for each hVps45 lysate. 400µL of Tlg2(1-309)-PrA, Sx16(1-280)-PrA, Tlg2(37-309)-PrA, Sx4-PrA, or Sx16(28-280)-PrA lysate per 5µL of beads was incubated for 1 hr at 4 °C while rotating, and the control beads incubated with 400uL of buffer per 5µL of beads. The beads were washed 3 times with 500µL of buffer and transferred to a clean tube. The beads were then incubated with 400µL of the wild-type, T224N, or E238K hVps45 lysate per 5µL of beads for 1 hr at 4 °C while rotating. The beads were washed with 500µL of lysis buffer and transferred to a clean tube. To elute bound protein, the beads were resuspended in 20µL of 2% SDS and vortexed on low for 10 min. The supernatant was then mixed with the appropriate amount of SDS-PAGE loading dye and heated at 70 °C for 10 min. The samples were visualized using Coomassie staining and Western blot.

Results

This project studied the interactions between Vps45 and its binding partner syntaxin, Tlg2 in yeast and Sx16 in mammals. Size-exclusion chromatography and native gel assays were performed with purified wild-type yVps45 and Tlg2(37-318), the truncation that does not contain the N-peptide, to directly test the binding mode involving the central cleft of Vps45 and Tlg2's closed conformation (Fig. 1C). Pulldown assays were performed to assess the binding of wild-type and mutant hVps45 to truncations of Tlg2 and Sx16.

To allow for the investigation of the wild-type interactions between yVps45 and Tlg2(37-318) for comparison to the two yVps45 mutants, the proteins was purified from *E. coli*. An existing bacterial expression plasmid was used to purify His-tagged wild-type yVps45 using affinity and anion-exchange chromatography. The proteins present throughout the purification process are shown in Fig. 2A, and the anion-exchange column chromatograph indicating the peak corresponding to yVps45 in Fig. 2B. The His-tagged Tlg2(37-318) purification process yielded similar results. In both cases, there was more contaminant chaperone protein than protein of interest following the Ni-NTA affinity purification, but the anion-exchange column allowed for a cleaner preparation, as shown in the penultimate lane of Fig. 2A compared to the last lane. To create the yVps45 mutations in the wild-type gene, site-directed mutagenesis was used. However, attempts to express and purify yVps45 mutants using these constructs were ultimately unsuccessful, possibly due to low expression or instability.

While troubleshooting mutant yVps45 expression from bacteria, binding assays were initially performed using the wild-type and Tlg2(37-318) to serve as a control for these methods to be used to investigate the mutants, as demonstrated in previous studies [7]. First, a size-

exclusion chromatography assay was performed to observe a potential shift resulting from the formation of a complex when the two proteins are incubated together. Fig. 3 shows the overlay of the UV chromatographs of wild-type yVps45 and Tlg2(37-318) run through the column individually or together. TCA precipitation was performed on the fractions corresponding to peaks to allow for visualization and identification of the proteins among the three runs on an SDS-PAGE gel. Both the chromatograph and gels show that both proteins shifted to earlier in the elution when incubated together in comparison to individually, indicating an increase in size and the formation of the complex.

Next, native gel assays were also performed to corroborate the results from size-exclusion chromatography. In these non-denaturing gels, interactions between proteins are preserved and the individual components are separated primarily based on differences in charge. To observe the formation of a complex, increasing concentrations of yVps45 with a fixed concentration of Tlg2(37-318) were incubated together and run on the gel. The proteins were run on the gel individually as well to allow for comparison to the location of the complex. The results of the individual and combined protein samples are shown in Fig. 4. The shift in the location of the band and the disappearance of the Tlg2(37-318) band (as shown in the second lane) as the concentration of yVps45 increases suggests binding. Together, the size-exclusion chromatography and native gel assays show detectable binding between yVps45 and Tlg2(37-318).

Since troubleshooting to express and purify the yVps45 mutants from bacteria was unsuccessful, the alternative strategy of overexpressing the protein in yeast was attempted. The mutant yVps45 genes created in this study were cloned from the bacterial expression plasmids into a yeast expression plasmid with a galactose-inducible promoter. An analytical digest of

clones following ligation is shown in Fig. 5. Since an additional EcoRV site would be introduced when the insert is present, all clones tested represent positive results, while the empty vector shows the result for a negative clone.

After confirmation by sequencing, small cultures of the yeast transformed with the mutant plasmids were induced to test for expression. Fig. 6A shows a Western blot of the two mutant proteins, but does not contain any definitive bands. Fig. 6B shows a Western blot from another attempt to express mutant yVps45 and includes expression of the SM protein Sec1 in the same plasmid backbone and strain of yeast as a positive control. Samples were also taken at different time points to investigate how long after exposing the yeast to galactose the genes were induced, as well as if the proteins were being degraded shortly after expression. Sec1 expressed well throughout the experiment, whereas there is no yVps45 visible at any of the time points.

Due to the absence of mutant yVps45 using bacteria or yeast, the human homolog of Vps45, which is conserved from yeast, was expressed instead using bacteria. To investigate the expression of the existing His-tagged constructs, wild-type hVps45, hVps45 T224N and hVps45 E238K were induced in a small-scale test. Fig. 7A shows expression from both 0.1mM IPTG and 1mM IPTG to optimize induction conditions. The expression was higher with 1mM IPTG, but the wild-type and mutants expressed similar amounts. The human homolog of Tlg2, Sx16, was also tested for expression. The construct initially used contains the full cytoplasmic portion of the A isoform of Sx16, including the N-peptide, and a C-terminal Protein A (PrA) tag, designated as Sx16(1-280)-PrA. This construct was used because the PrA tag recognizes rabbit IgG, which when conjugated to magnetic beads allow for proteins associated with Sx16(1-280)-PrA to be pulled out of lysate. For the initial test, IgG from a primary antibody made in rabbit

was used to detect the PrA tag of Sx16(1-280)-PrA after induction with 1mM IPTG. The results of this assay in Fig. 7B indicate that expression of Sx16(1-280)-PrA is detectable.

After confirming expression, a pulldown assay was performed to initially test the binding between Sx16(1-280)-PrA and both wild-type and mutant hVps45 in lysate without purifying each protein individually. Wild-type and mutant hVps45 lysate was incubated with both beads that had been incubated with Sx16(1-280)-PrA lysate and without Sx16(1-280)-PrA to determine if hVps45 bound to the beads nonspecifically or by associating with Sx16(1-280)-PrA. The results of this are shown in Fig. 8. The Sx16 blot shows similar amounts of Sx16(1-280)-PrA for the wild-type and mutants, allowing for a comparison of how much wild-type and mutant hVps45 is present based on affinity. Despite small differences in the amount of hVps45 present in the lysates between the wild-type and mutants and the potential for other proteins in the bacterial lysate to interfere with the interaction between hVps45 and Sx16, similar amounts were pulled down by Sx16, with less binding to the beads alone. This indicates that the full cytoplasmic portion of Sx16 appears to have comparable affinity to wild-type and mutant hVps45 at these concentrations.

A similar pulldown assay of hVps45 was performed with Tlg2(1-309)-PrA. Since the mammalian and yeast homologs have been shown to bind to each other, this would allow for a comparison to Sx16. Also, it would demonstrate that pulldowns with existing constructs of Tlg2 truncations and, in the future, with the yeast SNARE complex could be performed with the homologous hVps45 mutants. The results of this pulldown are shown in Fig. 9. Similar to the pulldown using Sx16(1-280)-PrA, the wild-type and mutants appear to bind to Tlg2(1-309)-PrA with similar affinity to each other under these conditions. Also, a consistent, low amount of non-specific binding was apparent without Tlg2(1-309)-PrA relative to the experimental lanes. The

faint, diffuse bands in the control lanes in the IgG blot detecting Tlg2(1-309)-PrA are likely due to the secondary antibody reacting with a small amount of IgG that was removed from the beads during the elution of the bound proteins. This also demonstrates binding between the yeast and human homologs.

In order to test the binding mode that involves the closed conformation of Tlg2/Sx16 and Vps45's central cleft independently of the mode involving the N-peptide of Tlg2/Sx16 and Vps45's hydrophobic pocket, pulldowns were performed using truncations of Tlg2/Sx16 without the N-peptide. The pulldown with Tlg2(37-309)-PrA was performed while creating the Sx16 construct without the N-peptide (Sx16(28-280)-PrA) and the results are shown in Fig. 10. Compared to the previous pulldowns, there is less hVps45 pulled down compared to the 10% lysate lanes. The experimental lanes show similar amounts of hVps45 to the background except for hVps45 E238K. However, this difference could be due to there being potentially less hVps45 E238K present in the lysate, especially in comparison to previous pulldowns. Despite this, there does appear to be a decrease in the amount of hVps45 E238K binding when Tlg2(37-309)-PrA is present when compared to the beads alone. This also shows that the binding between human and yeast homologs likely extends to truncations without the N-peptide.

To more directly test the mutated proteins, the Sx16 truncation lacking the N-peptide, Sx16(28-280)-PrA, was created. The gene without the sequence encoding the N-peptide was amplified using the Sx16(1-280)-PrA plasmid as a template and cloned back into the same plasmid as the vector to preserve the PrA tag. The results of the pulldown are shown in Fig. 11. As with Tlg2(37-309)-PrA, there is less hVps45 E238K in the experimental lane, but in this pulldown the amount of background is more consistent between the wild-type and mutants. Since wild-type hVps45 interacts with Tlg2/Sx16 without the N-peptide, improving the conditions of

the pulldown should show that the presence of hVps45 in the experimental lanes is due to specific binding.

For another negative control in addition to the beads without Tlg2/Sx16 shown in each experiment, syntaxin 4 ((Sx4)-PrA), a mammalian syntaxin SNARE that does not interact with Vps45, was used for the pulldown assay. The results are shown in Fig. 12. Unlike the previous pulldowns with truncations lacking the N-peptide, there is no decrease in hVps45 E238K in response to Sx4 binding to the beads. The amount of lysate for the E238K mutant appears to be more comparable to the other lysates in this case, in contrast to the Tlg2(37-309)-PrA and Sx16(28-280)-PrA pulldowns. Also, the binding in the experimental lanes appears to be similar to the background binding, with the exception of the first control lane that may have more signal due to its proximity to the adjacent lysate lane. This pulldown confirms that the amount of non-specific binding in the beads alone negative control is similar to the result when another protein that does not bind hVps45 is used and that this background is consistent between the wild-type and mutants.

Discussion

During this project, the interactions between both yeast and human Vps45 and their binding partners, Tlg2 and Sx16 respectively, were investigated. The binding between wild-type yVps45 and Tlg2(37-318) was confirmed by size-exclusive chromatography and native gel. The pulldown assay results suggest that there may be a difference in binding to Tlg2/Sx16 for at least one of the hVps45 mutants. However, improving the conditions of the pulldown assay and additional binding assays are needed to support this hypothesis. Overall, this project has demonstrated several assays that show binding between Vps45 and Tlg2/Sx16 and should be used to further characterize the Vps45 mutants.

The first finding is that the interactions between wild-type yVps45 and Tlg2(37-318) can be monitored qualitatively by native gel and size-exclusion chromatography assays, as shown in Fig. 3 and Fig 4. By varying the concentration of yVps45 and creating a binding curve based on the amount of Tlg2(37-318) bound or unbound, these or similar assays could be also used to measure affinity quantitatively. While these assays have been previously demonstrated [7], during this study various conditions have been tested to create useful protocols to be applied to the mutants. They demonstrate workable assays that can be used for either the yVps45 mutants or purified hVps45.

Another finding is that hVps45, both wild-type and mutant, can be successfully expressed in bacteria, is soluble when the cells are lysed, and interacts comparably with the full cytoplasmic portion of Tlg2 and Sx16. Fig. 7A shows hVps45 and Sx16(1-280)-PrA expression, and the results of the pulldowns (Fig. 8 and 9) show that they are soluble and functional due to their ability to associate. This binding is consistent with the two modes of association between

Vps45 its binding partners; the second mode of binding between the syntaxin's closed conformation and the central cleft of Vps45 (the area where the mutations are predicted to be located) could be disrupted, but the difference undetectable due to the binding of the N-peptide to Vps45's hydrophobic pocket.

This potential disruption was explored by pulldowns with Tlg2/Sx16 without the N-peptide, which suggest that there may be a difference in binding of hVps45 E238K to those truncations (Fig. 10 and 11). The lower amount of binding when compared to the full cytoplasmic syntaxins supports that the N-peptide and hydrophobic pocket is the preferred binding mode, but could also have been caused by the beads not being saturated with syntaxin resulting from lower expression in lysates for truncations without the N-peptide. Consequently, the amount of binding is too similar to the amount of non-specific binding to make conclusions. However, with both Tlg2(37-309)-PrA and Sx16(28-280)-PrA, there is a lower amount of the E238K mutant relative to the others, but it cannot be determined if the other mutant exhibits a detectable decrease. Furthermore, the Sx4-PrA negative control shows mostly consistent non-specific binding for the wild-type and mutants in both the beads alone and experimental samples. Together, these pulldowns suggest that there could be a decrease in affinity for Tlg2/Sx16 without the N-peptide when the E238K mutation is present, but standardizing the amount of protein used, improving the conditions of the control pulldown by blocking with BSA, and using more syntaxin should be done to support this hypothesis.

These possible interpretations of this study's results could be one potential explanation for the difficulties encountered when attempting to purify mutant yVps45. If the central cleft binding site is disrupted, the protein's structure could be disrupted as well, which could be more impactful in the yeast homolog. Initial purification of yVps45 from bacteria using the same

conditions as the wild-type yielded no detectable protein, and this occurred when mutant yVps45 was overexpressed in yeast as well (Fig. 6). This alternative approach was employed to attempt to promote proper folding using native chaperone proteins. This may indicate that the yVps45 mutants are less stable than the hVps45 homologs, or that the vectors for both bacteria and yeast are defective for reasons independent of the yVps45 genes.

Future studies should express mutant yVps45 in another vector to troubleshoot purification. Using the yeast homologs as opposed to the human versions provides several advantages. For example, interactions between the yeast homologs are better characterized, and several truncations of Tlg2 in addition to those used in this study already exist to explore how the yVps45 mutants may bind to them differently. In addition, the SNARE complex that Vps45 regulates is better characterized in yeast, as the identity of each protein is known. For example, yVps45 has been shown to bind to the v-SNARE Snc2, which is a component of the same SNARE complex as Tlg2. Assays such as those performed in this study could be used to compare binding of the wild-type and mutants to Snc2. In addition, assays of yeast SNARE complex binding and assembly *in vitro* can be performed. This could facilitate SNARE complex pulldown assays to test the effects of the mutations on yVps45's ability to bind to the SNARE complex or regulate SNARE assembly. Despite the absence of purifiable mutant yVps45, these results support previous research that has shown binding between the yeast and human homologs of Vps45 and Tlg2/Sx16 [10]. These assays also show that this association remains intact with Sx16/Tlg2 truncations and the hVps45 mutants, meaning that it is possible that the hVps45 mutants could be used to investigate binding to the yeast SNARE complex. Therefore, the results of this study have provided several avenues for testing the effects of Vps45 mutations on the SNARE complex.

Additionally, results from hVps45 and Sx16 analysis may be applied more directly to severe congenital neutropenia. Since this study has demonstrated successful expression and pulldown assays to test the interactions between hVps45 and Sx16, additional tests can be performed using improved conditions. hVps45 should be purified in order to allow for cleaner pulldown assays and standardization of the amount of protein incubated with the beads between the wild-type and mutants. In order to purify large amounts of Sx16, constructs without a PrA tag should be created, both with and without the N-peptide. Together, purified Sx16 and hVps45 could be used in the assays employed in this study for wild-type yVps45 and Tlg2(37-318) binding: size-exclusion chromatography and native gels. In addition, competition assays could be performed to compare the affinity of mutated hVps45 for the N-peptide and closed conformation of Tlg2/Sx16. These other binding assays could both corroborate results from the pulldown assays and, along with other methods, allow for more quantitative determinations of affinity, such as through electrophoretic mobility shift assays.

The results of these future studies could contribute to understanding the molecular mechanism of severe congenital neutropenia as caused by these two Vps45 mutations. After observing their effects *in vitro*, these mutations could be created in the endogenous yeast gene or on a plasmid transformed into a strain without Vps45 to observe potential sorting defects, as are present when Tlg2 is deleted [7]. These mutations should also be created in neutrophils and neutrophil progenitor cells to test if the mutations promote apoptosis of mature neutrophils or improper differentiation into neutrophils. The formation of granules and other markers of normal neutrophil function should also be monitored. This could suggest whether mutated Vps45 causes low neutrophil counts by interfering with regulated vesicle fusion, causing endoplasmic reticulum stress, or other mechanisms.

References

1. Bonifacino JS, Glick BS. The Mechanisms of Vesicle Budding and Fusion. Cell 2004;116(2):153-166.
2. De Matteis MA, Luini A. Mendelian Disorders of Membrane Trafficking. New England Journal of Medicine 2011;365(10):927-938.
3. Hong W, Lev S. Tethering the assembly of SNARE complexes. Trends in cell biology 2014;24(1):35-43.
4. Carr CM, Rizo J. At the junction of SNARE and SM protein function. Current Opinion in Cell Biology 2010;22(4):488-495.
5. Dulubova I, Yamaguchi T, Araç D, Li H, Huryeva I, Min S-W, Rizo J, Südhof TC. Convergence and divergence in the mechanism of SNARE binding by Sec1/Munc18-like proteins. Proceedings of the National Academy of Sciences 2003;100(1):32-37.
6. Carpp LN, Ciufo LF, Shanks SG, Boyd A, Bryant NJ. The Sec1p/Munc18 protein Vps45p binds its cognate SNARE proteins via two distinct modes. The Journal of Cell Biology 2006;173(6):927-936.
7. Furgason MLM, MacDonald C, Shanks SG, Ryder SP, Bryant NJ, Munson M. The N-terminal peptide of the syntaxin Tlg2p modulates binding of its closed conformation to Vps45p. Proceedings of the National Academy of Sciences 2009;106(34):14303-14308.
8. Stepensky P, Saada A, Cowan M, Tabib A, Fischer U, Berkun Y, Saleh H, Simanovsky N, Kogot-Levin A, Weintraub M and others. The Thr224Asn mutation in the VPS45 gene is associated with the congenital neutropenia and primary myelofibrosis of infancy. Blood 2013;121(25):5078.

9. Struthers MS, Shanks SG, MacDonald C, Carpp LN, Drozdowska AM, Kioumourtzoglou D, Furgason ML, Munson M, Bryant NJ. Functional homology of mammalian syntaxin 16 and yeast Tlg2p reveals a conserved regulatory mechanism. Journal of cell science 2009;122(13):2292-2299.

10. Dulubova I, Yamaguchi T, Gao Y, Min SW, Huryeva I, Südhof TC, Rizo J. How Tlg2p/syntaxin 16'snares' Vps45. The EMBO journal 2002;21(14):3620-3631.

11. Shanks SG, Carpp LN, Struthers MS, McCann RK, Bryant NJ. The Sec1/Munc18 protein Vps45 regulates cellular levels of its SNARE binding partners Tlg2 and Snc2 in Saccharomyces cerevisiae. PloS one 2012;7(11):e49628.

12. Welte K, Zeidler C, Dale DC. Severe Congenital Neutropenia. Seminars in Hematology 2006;43(3):189-195.

13. Vilboux T, Lev A, Malicdan MCV, Simon AJ, Järvinen P, Racek T, Puchalka J, Sood R, Carrington B, Bishop K and others. A Congenital Neutrophil Defect Syndrome Associated with Mutations in VPS45. New England Journal of Medicine 2013;369(1):54-65.

14. Theilgaard-Mönch K, Porse BT, Borregaard N. Systems biology of neutrophil differentiation and immune response. Current Opinion in Immunology 2006;18(1):54-60.

15. Boztug K, Klein C. Novel genetic etiologies of severe congenital neutropenia. Current Opinion in Immunology 2009;21(5):472-480.

16. Dale DC, Link DC. The Many Causes of Severe Congenital Neutropenia. The New England Journal of Medicine 2009;360(1):3-5.

17. Boztug K, Appaswamy G, Ashikov A, Schäffer AA, Salzer U, Diestelhorst J, Germeshausen M, Brandes G, Lee-Gossler J, Noyan F and others. A novel syndrome

with congenital neutropenia caused by mutations in G6PC3. The New England Journal of Medicine 2009;360(1):32-43.

18. Newburger PE, Dale DC. Evaluation and Management of Patients with Isolated Neutropenia. Seminars in hematology 2013;50(3):198-206.

19. Grenda DS, Murakami M, Ghatak J, Xia J, Boxer LA, Dale D, Dinauer MC, Link DC. Mutations of the ELA2 gene found in patients with severe congenital neutropenia induce the unfolded protein response and cellular apoptosis. Blood 2007;110(13):4179-4187.

20. Klein C, Grudzien M, Appaswamy G, Germeshausen M, Sandrock I, Schäffer AA, Rathinam C, Boztug K, Schwinzer B, Rezaei N. HAX1 deficiency causes autosomal recessive severe congenital neutropenia (Kostmann disease). Nature Genetics 2007;39(1):86-92.

21. Meerschaut I, Bordon V, Dhooge C, Delbeke P, Vanlander AV, Simon A, Klein C, Kooy RF, Somech R, Callewaert B. Severe congenital neutropenia with neurological impairment due to a homozygous VPS45 p. E238K mutation: A case report suggesting a genotype–phenotype correlation. American Journal of Medical Genetics Part A 2015;167(12):3214-3218.

Figures

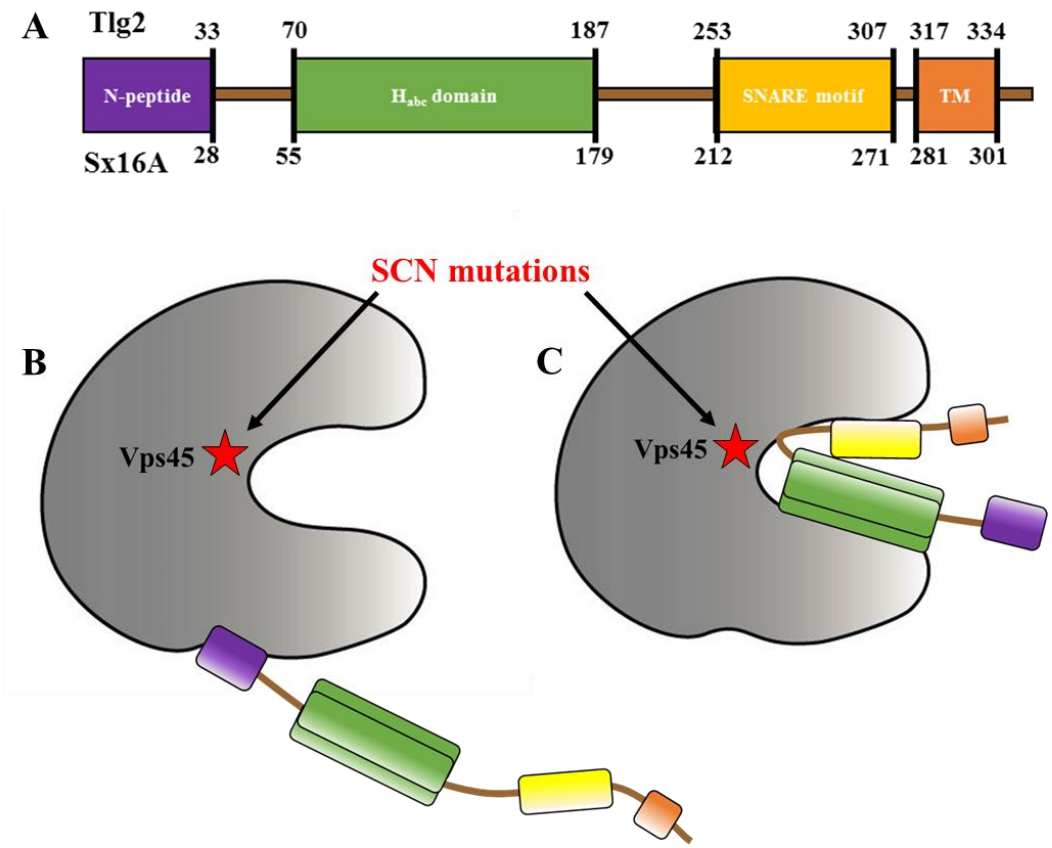

Figure 1: Tlg2/Sx16 domains and binding to Vps45*. **A)** Schematic of the conserved domains of Tlg2 and the A isoform of Sx16 with corresponding numbered residues: the N-terminal peptide, autoinhibitory H_{abc} domain, SNARE motif that participates in the SNARE complex's helical bundle and is inhibited by binding of the H_{abc} domain, and transmembrane region. **B)** Binding mode involving the N-peptide of Tlg2/Sx16 and the hydrophobic pocket on domain 1 of Vps45, which is the preferred binding site. **C)** Binding mode involving the closed conformation of Tlg2/Sx16 and Vps45's central cleft.*

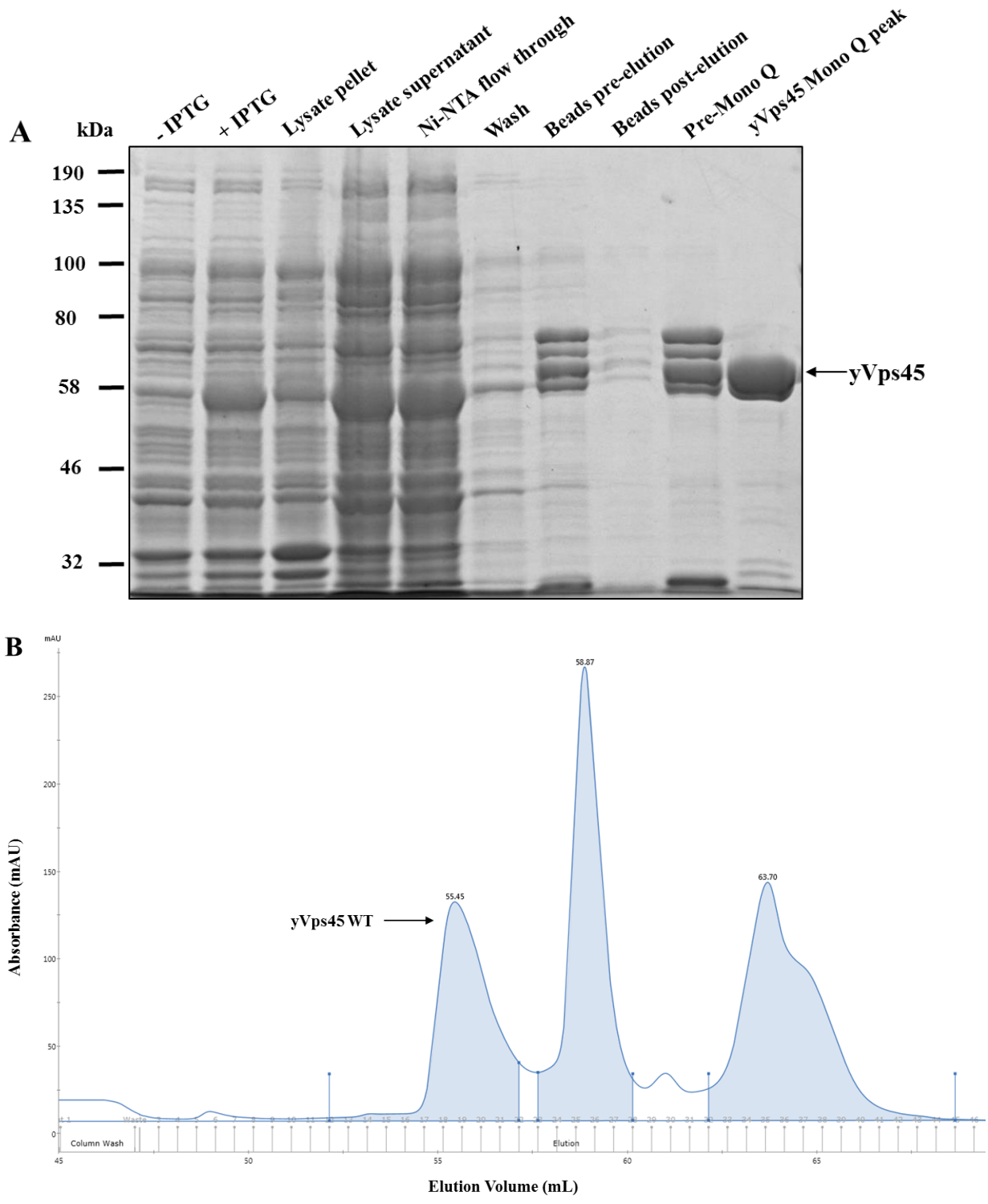

Figure 2: Wild-type yVps45 was purified from bacteria. A) *Samples taken throughout the purification process run on a 10% SDS-PAGE gel. Arrow indicates yVps45 at expected size of 67 kDa.* ***B)*** *UV chromatograph of protein absorbance at 280nm from Mono Q 5/50 GL (GE) gradient elution, indicating the yVps45 peak.*

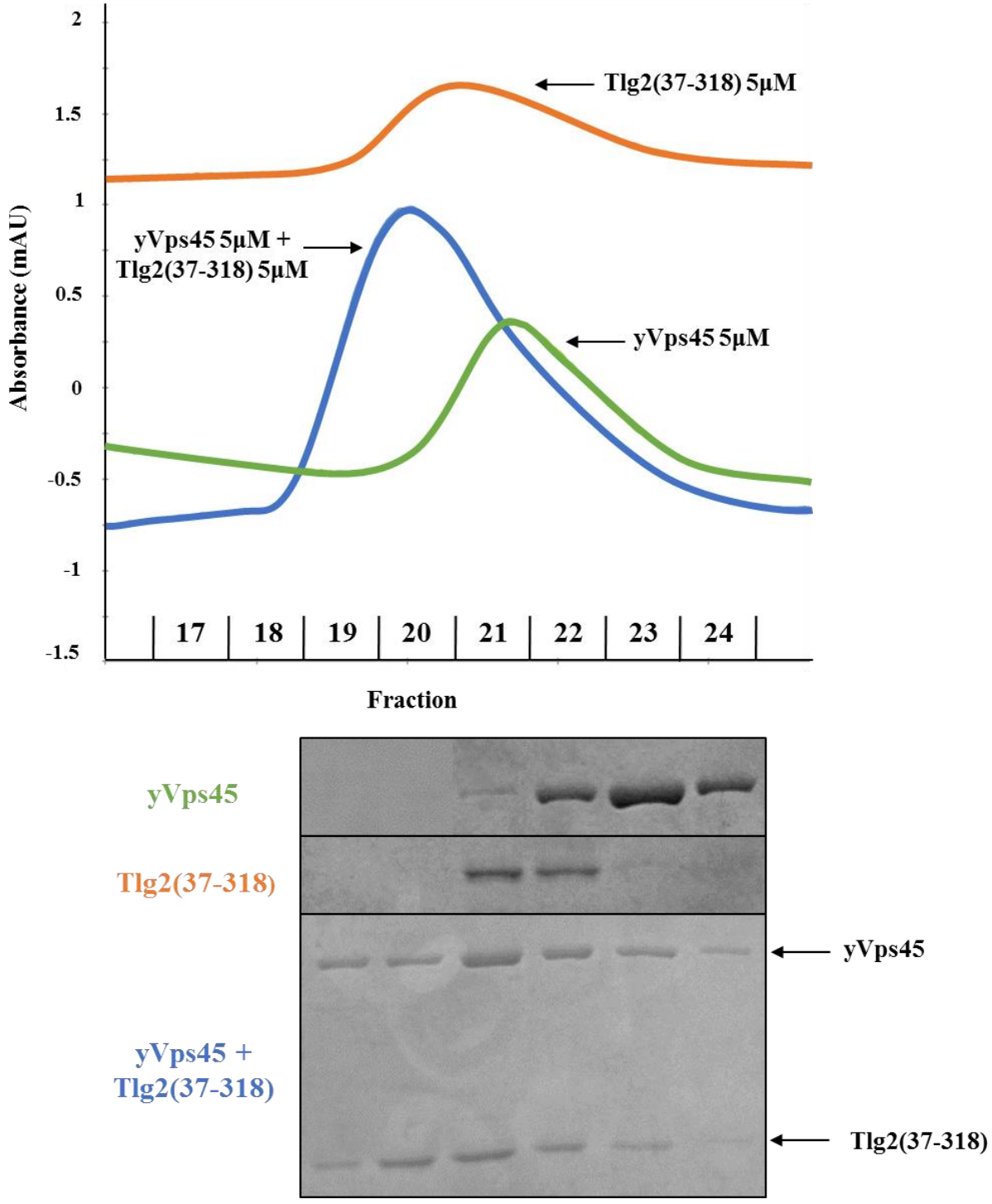

Figure 3: Size-exclusion chromatography shows wild-type yVps45 binding to Tlg2(37-318). *Samples of 5µM yVps45 and Tlg2(37-318) were applied to the GE Superdex 200 10/300 GL column separately and then after being incubated together. The UV chromatograph detecting protein by absorbance at 280nm overlays all three runs. 10% SDS-PAGE gels were run to visualize the contents of the fractions corresponding to each peak using Coomassie staining. Each lane contains results from the corresponding fraction number in the above chromatograph.*

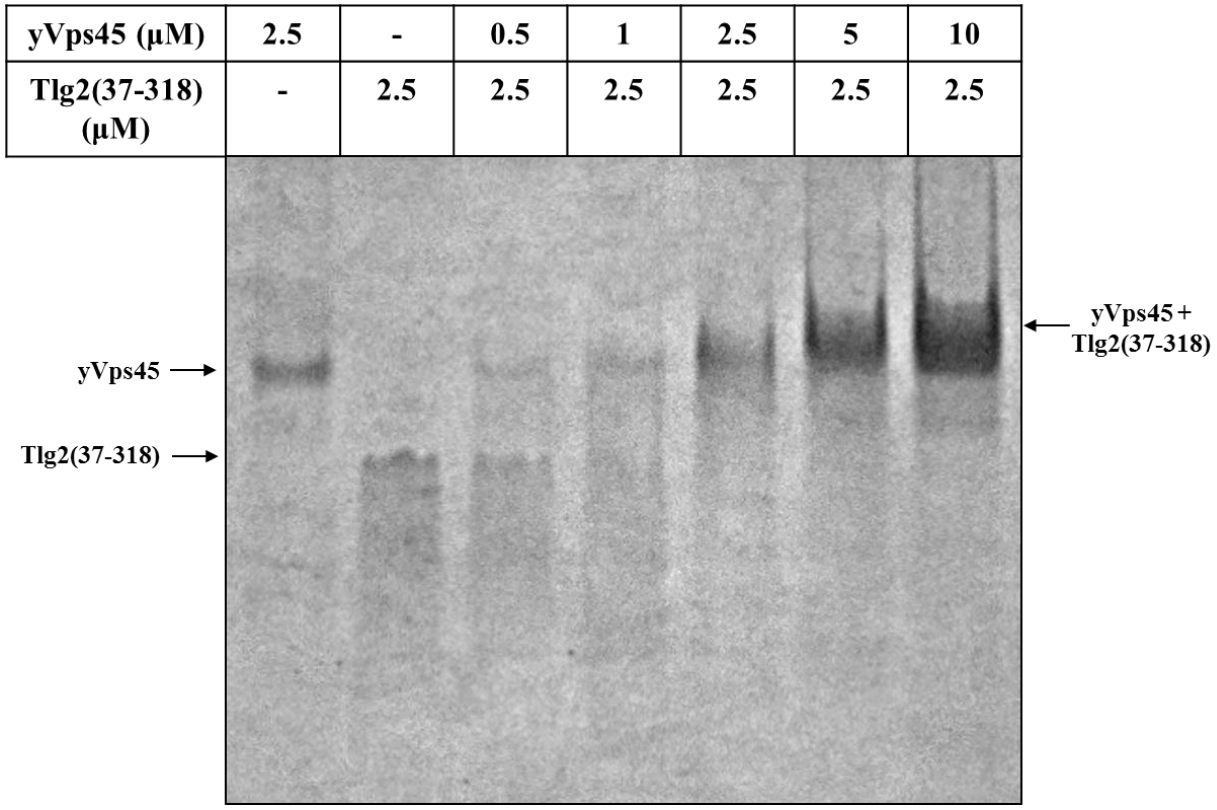

Figure 4: Native gel assay shows wild-type yVps45 binding to Tlg2(37-318). *Increasing concentrations of yVps45 were incubated with 2.5μM Tlg2(37-318) for 45 min, as well as 2.5μM samples of each protein individually. All samples were run on a 6% native gel at constant amperage of 30mA for 90 min and the proteins visualized by Coomassie staining.*

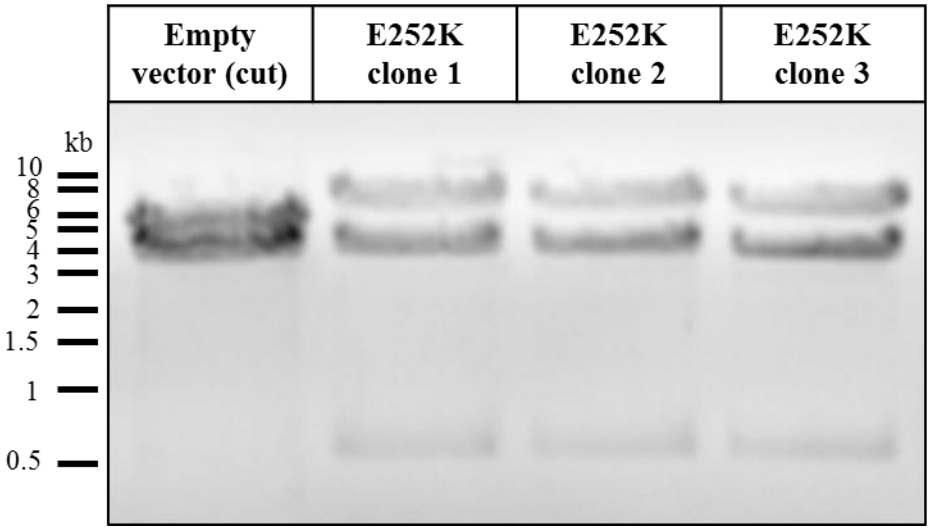

Figure 5: yVps45 E252K cloning analytical digest. *0.8% agarose gel of digestion with EcoRV of empty cut vector and three yVps45 E252K clones after ligation. Expected sizes of fragments for positive clones (kb): 0.4, 3, and 4.9. Expected sizes of fragments for negative clones (kb): 2.8 and 3.8.*

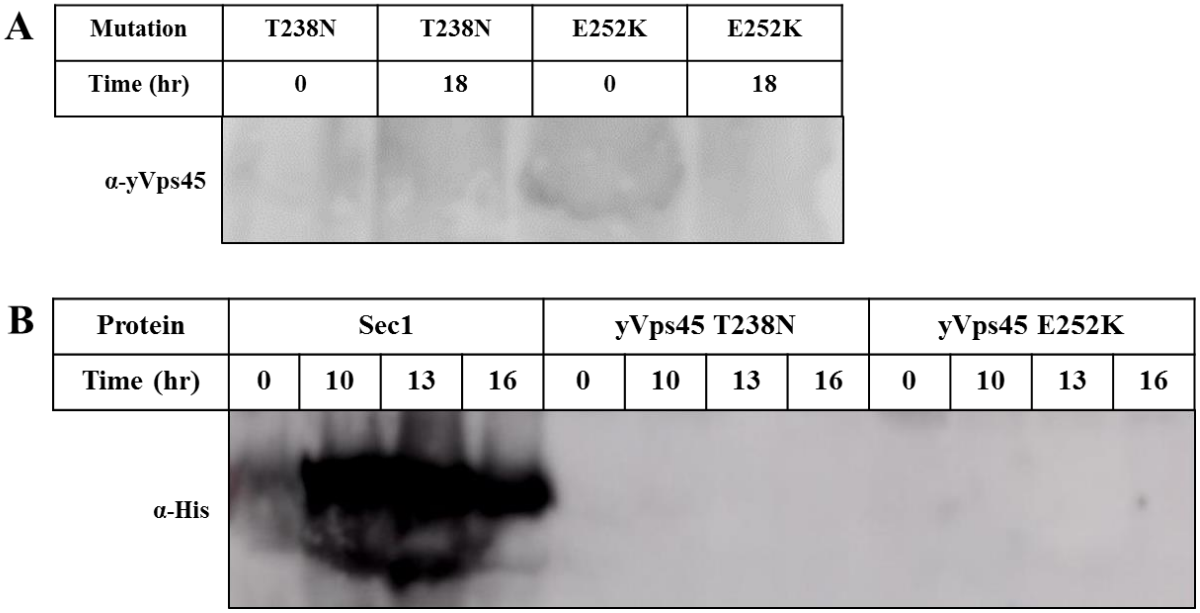

Figure 6: Small-scale tests of mutant yVps45 overexpression in yeast showed no detectable protein. A) *Western blot of mutant yVps45 expression before and after induction. A yVps45 antibody (mouse) was used and the blot was exposed for 2 min.* ***B)*** *Western blot of mutant yVps45 expression at multiple time points after induction with the SM protein Sec1 as a positive control. A His-tag antibody (mouse) was used and the blot was exposed for 30 sec.*

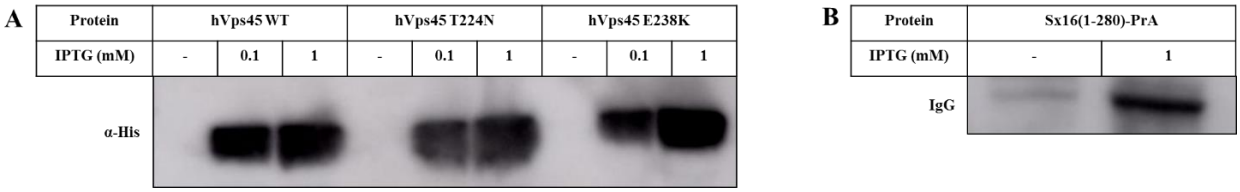

Figure 7: Small-scale tests of hVps45 and Sx16(1-280)-PrA in bacteria yielded expression*. A)* *Western blot of a small-scale induction test of hVps45 expressed using bacteria was completed first to test for mutant hVps45 expression before proceeding further. Samples were taken before cultures were induced with either 0.1mM or 1mM IPTG and after 18 hr to determine induction conditions to be used. A His-tag antibody (mouse) was used. The blot was exposed for 1 min.* ***B)*** *Western blot of a small-scale induction test of Sx16(1-280)-PrA was performed as well. Rabbit IgG from a Sec1 antibody was used to recognize the C-terminal PrA tag. The blot was exposed for 15 sec.*

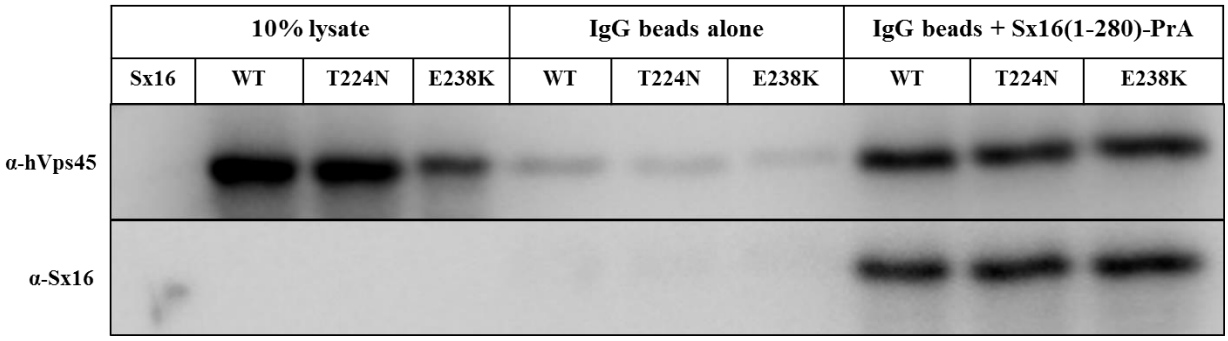

Figure 8: hVps45 WT, T224N, and E238K interact comparably with Sx16(1-280)-PrA. *Western blots of hVps45 WT, T224N, and E238K pulldowns with Sx16(1-280)-PrA were performed. A hVps45 antibody (rabbit) was used and the blot exposed for 10 sec. A Sx16 antibody (rabbit) was used and the blot exposed for 10 sec.*

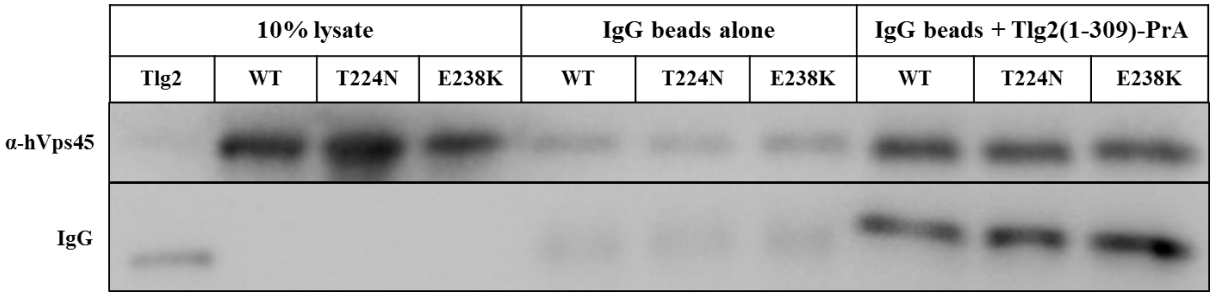

Figure 9: hVps45 WT, T224N, and E238K interact comparably with Tlg2(1-309)-PrA. *Western blots of hVps45 WT, T224N, and E238K pulldowns with Tlg2(1-309)-PrA were performed. A hVps45 antibody (rabbit) was used and the blot exposed for 10 sec. Rabbit IgG from a Sx16 antibody was used to detect the PrA tag on Tlg2(1-309)-PrA and the blot exposed for 1 sec.*

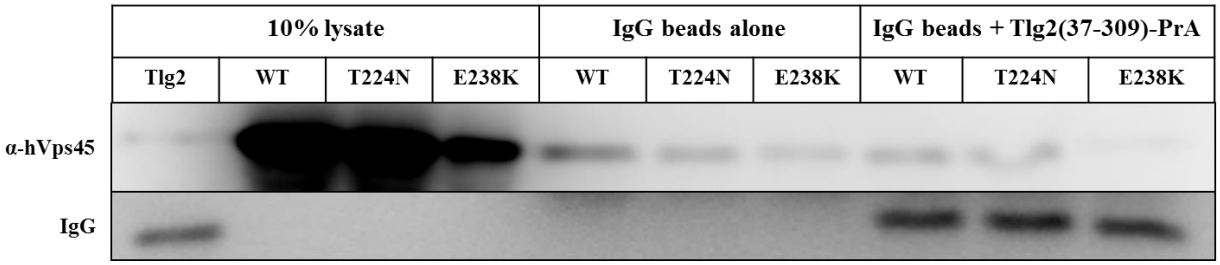

Figure 10: Mutant hVps45 may associate less strongly with Tlg2(37-309)-PrA. *Western blots of hVps45 WT, T224N, and E238K pulldowns with Tlg2(37-309)-PrA were performed. A hVps45 antibody (rabbit) was used and the blot exposed for 30 sec. Rabbit IgG from an Sso1 antibody was used to detect the PrA tag on Tlg2(37-309)-PrA and the blot exposed for 1 min.*

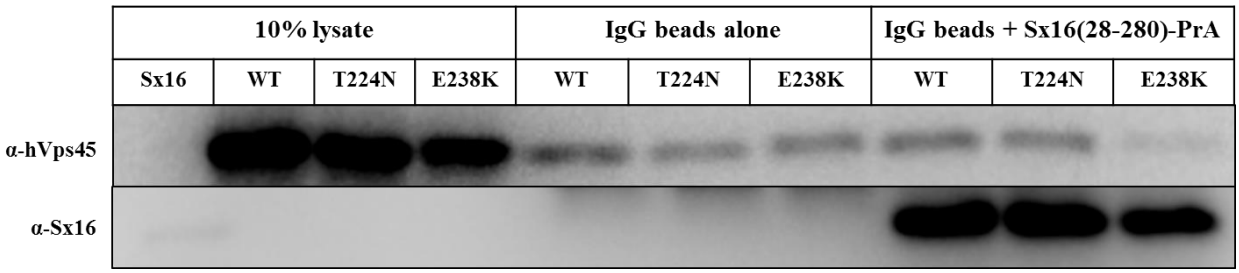

Figure 11: Mutant hVps45 may associate less strongly with Sx16(28-280)-PrA. *Western blots of hVps45 WT, T224N, and E238K pulldowns with Sx16(28-280)-PrA were performed. A hVps45 antibody (rabbit) was used and the blot exposed for 1 sec. A Sx16 antibody (rabbit) was used and the blot exposed for 2 min.*

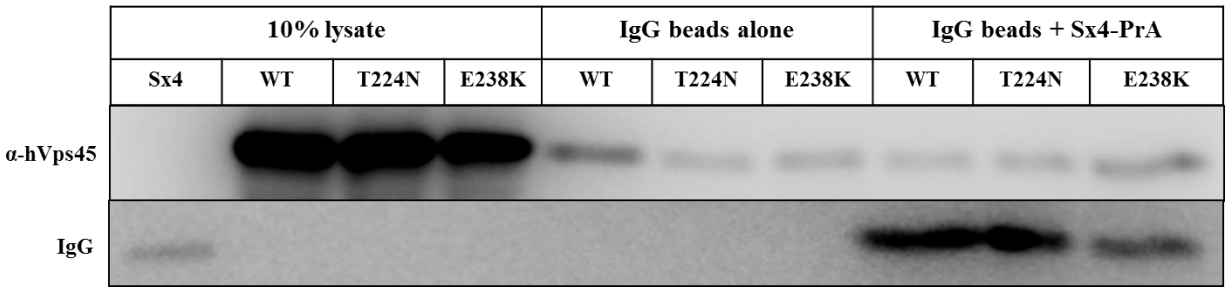

Figure 12: hVps45 WT, T224N, and E238K pulldowns with Sx4-PrA shows binding similar to background binding. *Western blots of hVps45 WT, T224N, and E238K pulldowns with Sx4-PrA, a syntaxin that does not interact with hVps45, were performed. A hVps45 antibody (rabbit) was used and the blot exposed for 10 sec. Rabbit IgG from an Sso1 antibody was used to detect the PrA tag on Sx4-PrA and the blot exposed for 5 sec.*